J Mater Sci (2011) 46:5723–5731
DOI 10.1007/s10853-011-5526-4

Hybrid organic/inorganic composites based on silica and weak synthetic polyelectrolytes

Marcela Mihai · Ecaterina Stela Drăgan

Received: 7 February 2011 / Accepted: 4 April 2011 / Published online: 13 April 2011

Abstract The preparation and characterization of new organic/inorganic composites by the consecutive adsorption of weak polyelectrolytes on silica particles were studied in the article. Two polycations containing primary amine groups in the side chains, poly(vinylamine) or poly[*N*(*β*-aminoethylene) acrylamide], and poly(acrylic acid) as polyanion were used for the hybrid materials construction. The stability of the organic/inorganic composites has been increased by a heat-induced reaction at 150 °C. The organic/silica hybrids properties were monitored by potentiometric titration, laser light scattering, infrared spectroscopy, and thermogravimetric analysis. The adsorption of methylene blue by the composite materials has been tested. The dye adsorption capacity was strongly influenced by the dye concentration, the nature of the last adsorbed layer, the polyions concentration, and the composite thermal treatment.

Introduction

Micro- and nano-scale control of the organic/inorganic materials structure is a prerequisite for the fabrication of sophisticated functional devices [1–4]. The layer-by-layer (LbL) assembly of polyelectrolytes has emerged last years as a particularly versatile method to fabricate functional multilayered films [5, 6]. LbL technique, which exploits the electrostatic attraction between oppositely charged species alternately adsorbing on a surface from solution, has been used to prepare films on substrates with different shapes and sizes [7–10], using a variety of compounds, such as synthetic polyelectrolytes and biological macromolecules [3, 5, 11], dyes [12], nanoparticles [4, 10, 13], carbon nanotubes [14], etc. Other types of interactions than the electrostatic one, notably H-bonding [15] or specific complexation [16], have been demonstrated to be useful for LbL assembly, thereby widening further the applicability of the method. Choosing the appropriate compounds enables the fabrication of functional films for various applications, e.g., in biotechnology for preparing polyelectrolyte–protein multilayer films [17], in separation applications [18], catalysis [19], chemical sensors [20], ultrathin ion-selective membranes [11, 21], and electrochromic devices [22].

While the multilayer thin films were originally formed from strong polyelectrolytes, increasing attention has been paid last years to multilayers consisting of weak polyelectrolytes [7, 11, 23–25]. The pH dependent dissociation of weak polyelectrolytes can modulate the reactivity of the resulting multilayer thin film, tuning the fraction of the reactive groups, which are involved in the polyelectrolyte inter-layer complexation. Furthermore, structural changes in the layer architecture of such multilayers can be induced by changes in the environmental pH to produce microporous thin films. Heat-induced reactions involving two functional groups proved to be an interesting route in the formation of covalent bonds in the electrostatically or H-bonds stabilized polyelectrolyte multilayers [8, 26] or polyelectrolyte complexes [27]. Primary or secondary amine groups from polycations, on the one hand, and carboxylic groups from polyanion, on the other hand, may be involved in heat-induced reactions with the transformation of the ammonium–carboxylate ion pairs into amide bonds by heating at appropriate temperatures (150–180 °C).

M. Mihai (✉) · E. S. Drăgan
"Petru Poni" Institute of Macromolecular Chemistry,
Grigore Ghica Vodă Aleey 41 A, 700487 Iaşi, România
e-mail: marcelas@icmpp.ro

The objectives of this study were the preparation and characterization of some organic/inorganic composites by the consecutive adsorption of weak polycation and weak polyanion onto silica particles. For the organic/inorganic composites construction, two polycations containing primary amine groups in the side chains, poly(vinylamine) (PVA) or poly[*N*(*β*-aminoethylene) acrylamide] (PAEA), and poly(acrylic acid) (PAA) as polyanion have been used. The possibility to transform the amine–carboxylic H-bonds into amide groups, by a heat-induced reaction, annealing the organic/silica composites at 150 °C, has been discussed. The organic/inorganic composite properties were deeply investigated by potentiometric titrations, FT-IR spectroscopy, laser diffraction scattering, and thermogravimetric analyses (TGA). The adsorption of methylene blue (MB) on the composite materials has been tested as a function of the dye concentration, the nature of the last adsorbed polymer, the polyions concentration, and the composites thermal treatment.

Experimental

Materials

Silica particles, with a mean diameter ranged between 30 and 50 μm, particles surface area 150 $m^2\ g^{-1}$ and the average pore radius, r_p, 30 nm, were used as inorganic substrate material.

PVA with a degree of hydrolysis of 95 mol% and a molar mass of $M_w = 40000\ g\ mol^{-1}$ was provided by BASF (Ludwigshafen, Germany). PAEA was synthesized by the aminolysis–hydrolysis reaction of polyacrylonitrile with ethylenediamine, according to the method previously presented [28]. The intrinsic viscosity of this polymer, determined in 0.1 M NaCl at 25 °C, was $[\eta] = 0.1645$ dL g^{-1}. PAA with $M_w = 61000\ g\ mol^{-1}$ (Polysciences Inc) was used as received. MB from Aldrich was used without further purification. The structures of the polyions used in the multilayer construction and of MB are presented in Fig. 1.

Methods

Preparation of organic/silica composites by LbL adsorption

The concentration of the aqueous solutions of polyelectrolytes was either 5×10^{-2} M or 10^{-2} M. Polymers adsorption was carried out at room temperature, for 1 h every layer, under gentle shake. After every adsorption step, the organic/silica particles were washed three times with distilled water (pH = 5.5) to rinse the weakly adsorbed polymer from the particles surface. The procedure has been repeated until the desired number of layers was achieved. The composite materials were not dried between the adsorption steps. After the organic/inorganic hybrid formation, part of the composite material was annealed 1 h at 150 °C, in the oven, to stabilize polymer layers by a heat-induced reaction.

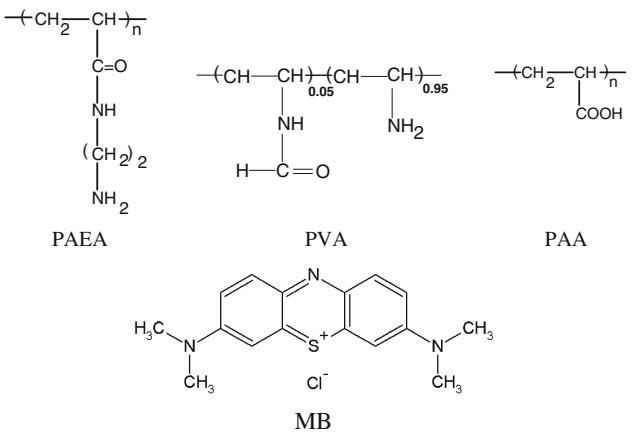

Fig. 1 Chemical structure of the polyelectrolytes and methylene blue

Organic/inorganic composites characterization

Potentiometric titrations were performed with the particle charge detector PCD 03 (Mütek™ GmbH, Germany), between pH 2.5 and 10, using 0.1 mol L^{-1} HCl or NaOH, respectively.

Measurement of organic/silica hybrids size has been performed using laser diffraction technology, with a Mastersizer 2000 system (version 5.31) (Malvern Instruments, Malvern, England). The system is constituted of an optical bank which uses laser light He–Ne 632 nm/2 mW, a dispersion unit of the sample Hydro 2000A-type equipped with stirrer, recirculation pump, ultrasonic system, and software to record and process results on the computer, using the Mie theory [29]. This theory is based on the assumption that particles are homogeneous and spherical, the optical properties of particle and dispersion medium are known, and suspension dilution guarantees that light scattered by one particle is measured before being re-scattered by other particles.

FTIR spectra of organic/inorganic composites were recorded with a DIGILAB spectrometer Scimitar Series, USA, resolution of 4 cm^{-1}, in the range of 4000–400 cm^{-1}, by KBr pellet technique.

Thermogravimetric analyses, for all samples under study, were performed on 50 mg sample at a heating rate of 9 °C min^{-1} up to 500 °C, DTG sensitivity of 1/10, in air, using a Paulik-Paulik-Erdey Derivatograph, Budapest; α-Al_2O_3 was used as the reference material.

Dye adsorption on organic/inorganic composites

The study of the dye adsorption properties of the organic/inorganic composites was carried out using a batch equilibrium procedure. Thus, 25 mg of dry composite material was placed in a flask and contacted with 10 mL of aqueous solution of MB with different concentrations under gentle shake at room temperature for 8 h. The residual concentration of MB remained in the supernatant was determined using a SPECORD M42 spectrophotometer by measuring the absorbance in the supernatant at 665 nm. The color removal efficiency, CRE (%), of the composite materials was calculated according to Eq. 1:

$$\text{CRE}\ (\%) = (1 - A_c/A_i) \times 100 \quad (1)$$

where A_i and A_c are the absorbance of the dyes before and after the adsorption process, respectively.

Results and discussion

The formation of organic/inorganic composite materials took place by the consecutive deposition of the complementary polyelectrolytes, by interaction of polycations containing primary amine groups and the polyanion, which contains carboxylic groups. In aqueous solution, the polycations PVA and PAEA and the polyanion PAA had different pH, namely about 9.6, 10.2, and 3.5, at concentrations of 10^{-2} M, respectively, and a coiled conformation due to a small degree of ionization [30, 31]. Thus, it is expected as the main interactions between layers to be as H-bonds. Part of the organic/silica hybrids has been heated at 150 °C following the feasibility of a heat-induced reaction of the amine–carboxylic pairs into amide bonds.

Streaming potential versus pH

Although the value of streaming potential depends on numerous factors and can not be used as an absolute value (in the same way as ζ-potential), the method of colloidal titration with streaming potential detection is useful to determine the point of zero charge (*pzc*) of polyelectrolytes in solutions and of colloidal dispersions. The *pzc* is considered the value of pH where the streaming potential, Ψ, is 0 mV. Figure 2 shows the variation of the streaming potential as a function of pH for silica and $(PAEA/PAA)_2$/silica particles, with polyions adsorbed at different concentrations.

The variation of streaming potential as a function of pH gives information on changes of the silica surface charge after the adsorption of oppositely charged polyions. Thus, potentiometric titrations in water showed that *pzc* was reached at pH = 2.53 for bare silica (Fig. 2). Above this

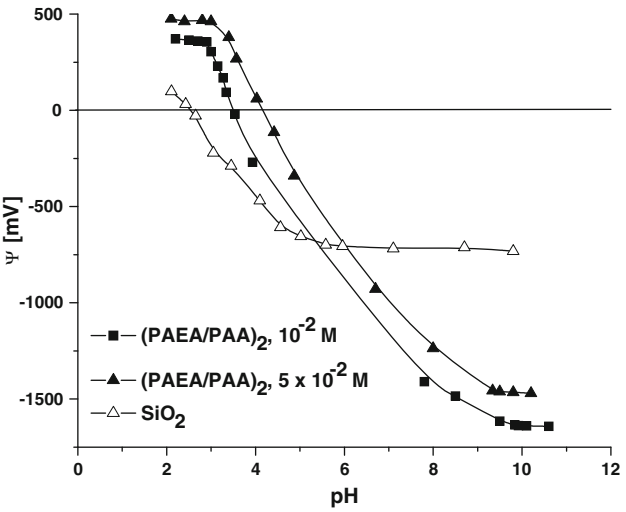

Fig. 2 The variation of the streaming potential versus pH for silica and $(PAEA/PAA)_2$/silica particles with polyions adsorbed at two different concentrations

value, the surface of silica particles suspended in water is negatively charged, due to the silanolate ions ($Si–O^-$). In the presence of hydronium ions, the primary amino groups of polycations PAEA and PVA can be protonated ($–NH_3^+$), and the carboxyl groups of PAA can be dissociated in $–COO^-$ in the presence of hydroxyl ions. Previous studies showed that *pzc* is located at pH = 9.2 for PAEA [30], at pH = 10.2 for PVA [31], and at pH = 2.2 for PAA [31]. Due to the polyions adsorption on silica particle surface and their intrinsic contribution to the overall *pzc* of the hybrid materials, an increase of *pzc* at pH = 3.46 for $(PAEA/PAA)_2$/silica hybrids, with polyions adsorbed from 10^{-2} M aqueous solution, was evidenced. Moreover, *pzc* increased at pH = 4.16 with the increase of the concentration of the adsorption solutions (5×10^{-2} M), suggesting the increase of the amount of adsorbed polymers.

FT-IR spectroscopy

The formation of multilayer thin films was also monitored by FT-IR spectra performed on bare silica particles, and on the $(PAEA/PAA)_2$/silica particles, with polyions adsorbed from 10^{-2} M aqueous solutions, before and after the thermal treatment (Fig. 3). To demonstrate the formation of amide bonds during the thermal treatment, Fig. 3 contains also the spectra of the same composite samples after immersion in 2 N HCl for 24 h.

In Fig. 3, the FTIR spectrum of the bare silica particles shows the following characteristic bands: 1620 and 810 cm^{-1}, assigned to Si–OH groups, 1101 cm^{-1} assigned to Si–O–Si groups, and 1398 cm^{-1} assigned to $Si–O^-$ groups [32]. After the multilayer deposition, the band at

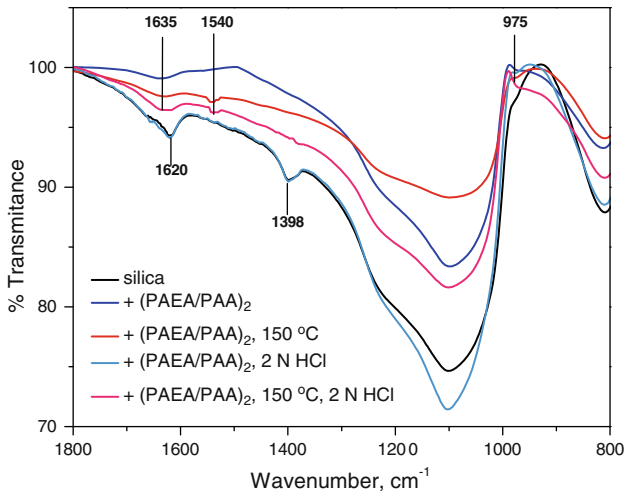

Fig. 3 FT-IR spectra of bare silica particles and of the (PAEA/PAA)$_2$/silica particles with polyions adsorbed from 10^{-2} M aqueous solutions before and after thermal and HCl treatment

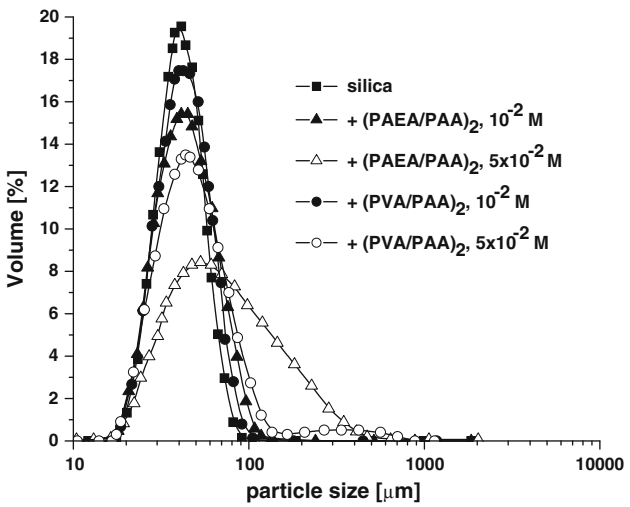

Fig. 4 The particle size distribution, as volume fraction versus particle diameter for silica particles before and after the polyelectrolyte multilayer adsorption

1398 cm^{-1} disappears, due to the surface coverage with polyelectrolyte multilayer, and some characteristic bands of pure PAEA sample can be observed, such as 1635 (amide I) and 975 cm^{-1} (–NH_3^+). In the spectrum of (PAEA/PAA)$_2$/silica, after the thermal treatment at 150 °C, the absorption band at 975 cm^{-1} disappears while the amide I band at 1638 cm^{-1} increased and a shoulder at 1540 cm^{-1} (amide II) appears, suggesting that after the thermal treatment the ion pairs were transformed into covalent bonds. Similar characteristics were observed in the spectra of (PVA/PAA)$_2$/silica before and after the thermal treatment (data not shown here).

After immersion of samples in 2 N HCl, for 24 h, the FTIR spectra evidenced the destruction of the electrostatic-based multilayer coverage on the silica surface, whereas the spectrum of the thermal treated composite material is very similar with that recorded on the sample before the acid treatment. These results suggest that after thermal treatment the layers became more stable due to the covalent crosslinkages between complementary polyions by amide bond formation.

Laser diffraction scattering

In order to obtain more information about the influence of the polycation structure and polyions concentration on the composite characteristics, measurements of composite particles size as well as of the bare silica particles were performed. The particle size distribution, as volume fraction versus particle diameter, as average of three independent measurements, is shown in Fig. 4. For each sample, the average values of standard quantities $d(0.1)$, $d(0.5)$, and $d(0.9)$ (the particles mean size of less than 10, 50, and 90 vol% of the particles under study, respectively) and polydispersity index (PI) (the width of the particles size distribution, based on the 10 vol.%, 50 vol.% and 90 vol.% quantile) were included in Table 1.

The bare silica particles show a unimodal distribution in particle size (PI = 0.8), the medium diameter, given as $d(0.5)$ value [$d(0.5)$ is the mass median diameter], being 40.7 ± 1.04 μm. After the adsorption of two double layers (polycation/PAA) on silica particles, the concentration of adsorbed polyions being 10^{-2} M, the distribution of the particle sizes ranged between ~20 and 110 μm, and the $d(0.5)$ value increased irrespective of the polycation structure. The highest $d(0.5)$ value was observed when PAEA was the polycation (48.5 ± 1.26 μm), i.e., the polycation with a longer spacer between the polymer backbone and the ammonium groups, comparative with (PVA/PAA)$_2$/silica [$d(0.5)$ 42.6 ± 1.13 μm]. Moreover, PI values lower than 1.0, obtained for composites prepared at the concentration of adsorbed polyions of 10^{-2} M, suggest that during adsorption process no particles aggregation occurred. Increasing the polyelectrolyte concentrations, the charges along the polyelectrolyte chain become more screened, leading to an enhanced coiling of the chains and an increase in the adsorbed amount and layer thickness. Thus, increasing the polyions concentration to 5×10^{-2} M, the mean particles size increased up to $d(0.5)$ ~ 63.2 ± 1.84 μm when PAEA was used as polycation, an aggregation tendency of the hybrid particles being evident at this concentration, PI being 1.1 and 2.17 when PVA and PAEA were used, respectively.

To explain the high thickness of the shell, even at the lower polyions concentration, the adsorption condition of complementary polyelectrolyte must be considered, and Scheme 1 was imaged to suggest the process which took place.

Table 1 Particle size distribution of silica particles before and after multilayer deposition

Sample	Polyions concentration (M)	Particles diameter (μm)			
		$d(0.1)^a$	$d(0.5)^b$	$d(0.9)^c$	PI[d]
Silica particles		26.9 ± 0.54	40.7 ± 1.04	59.5 ± 1.68	0.800
+$(PVA/PAA)_2$	10^{-2}	27.5 ± 0.55	42.6 ± 1.13	65.3 ± 1.85	0.887
+$(PVA/PAA)_2$	5×10^{-2}	28.0 ± 0.56	47.7 ± 1.21	80.6 ± 2.31	1.102
+$(PAEA/PAA)_2$	10^{-2}	29.6 ± 0.61	48.5 ± 1.26	72.7 ± 2.02	0.889
+$(PAEA/PAA)_2$	5×10^{-2}	36.4 ± 0.72	63.2 ± 1.84	173.6 ± 4.52	2.171

[a] The particles diameter determined at the 10th percentile of undersized particles

[b] The mass median diameter, the particles diameter determined at the 50th percentile of undersized particles

[c] The particles diameter determined at the 90th percentile of undersized particles

[d] Polydispersity, the width of the particles size distribution, PI = $[d(0.9) - d(0.1)] \div d(0.5)$

In the first adsorption step, the polycation had a coiled conformation due to its small degree of ionization (pH of the adsorption solution of about 9.6). Thus, during the adsorption process, polycation coils cover the surface with a thick layer (Scheme 1, step I). When the polycation/silica particles were immersed into the washing solution (distilled water, pH = 5.5), the protonation of part of amino groups occurs, which determines the extension of the polycation chains (Scheme 1, step II). The extended polycation chains preserved this conformation in the next adsorption step, at pH = 3.5, and thus were able to catch a large number of PAA coils (Scheme 1, step III). In the next washing step, PAA will become highly ionized, due to the pH changes at 5.5, which conduct to the extension of the polyanion chains (Scheme 1, step IV), this process having two consequences: the removal of polyanion chains in excess and catching polycation coils in the next adsorption step. Thus, a highly interpenetrated network is expected to be formed and a fast growth of the film thickness.

Thermogravimetric analysis

Thermal degradation is frequently used in the study of polymers from the theoretical and practical point of view, as sensitive method to follow water loss by physical or chemical processes [27, 33]. In this study, we have investigated the effect of polyelectrolyte structure on the thermal stability of organic/silica particles before and after the thermal treatment. TGA data of some organic/silica composites are presented in Fig. 5.

Table 2 includes the following parameters, determined for each decomposition step: the initial decomposition temperature (°C), T_i, the temperature corresponding to the maximum rate of decomposition (°C), T_m, the final

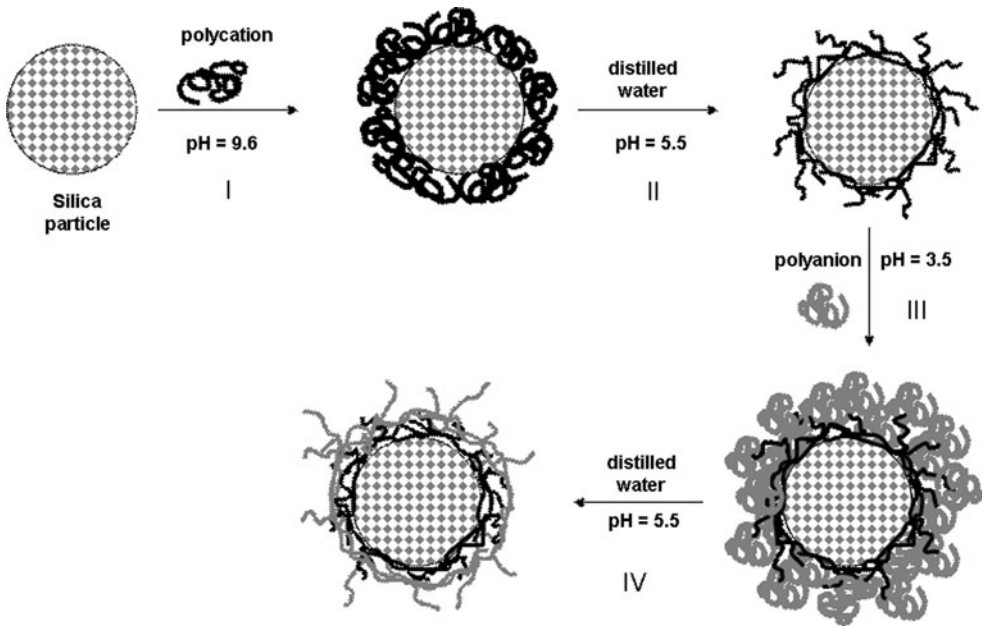

Scheme 1 Schematic representation of organic/silica composites formation

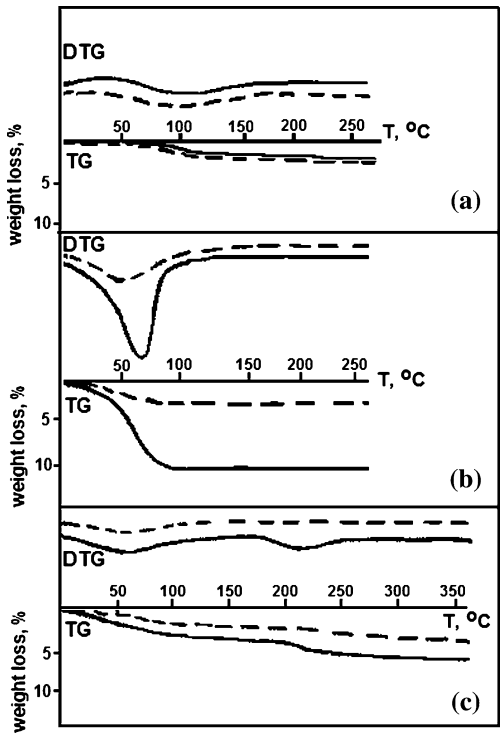

Fig. 5 TGA curves of some multilayer/silica samples before (straight line) and after (dashed line) the thermal treatment: **a** $(PAEA/PAA)_2$, 10^{-2} M; **b** $(PVA/PAA)_2$, 10^{-2} M; and **c** $(PVA/PAA)_2$, 5×10^{-2} M

temperature (°C), T_f, the weight loss, w, (%), and the global kinetic parameters calculated by Coats and Redfern method [34], namely, the reaction order, n, and the activation energy (kJ mol^{-1}), E_a.

Among the known integral methods, the most commonly used in the kinetic analysis of thermal decomposition of various materials is the integral method proposed by Coats and Redfern [35–37]. The method assumes various orders of reaction and compares the linearity in each case to select the correct order. The activation energy was determined using the Eq. 2:

$$\log \frac{F(\alpha)}{T^2} = \log \left[\frac{A}{a} \frac{R}{E_a} \left(1 - \frac{2RT}{E_a} \right) \right] - \frac{E_a}{2.3R} \frac{1}{T} \quad (2)$$

where T is the temperature, a is the heating rate, E_a is the activation energy, A is the pre-exponential factor, α is the conversion degree, and R is the universal gas constant. The value of the reaction order was determined by tests of the function form $F(\alpha)$, so that the graphical representation $[\log F(\alpha)/T^2]$ versus $[1/T]$ should be linear, and the activation energy was obtained from the slope of the line obtained in this way.

The TGA curves for all composite samples prepared in the article (Fig. 5) show a degradation stage between 50 and 150 °C, the maximum rate of decomposition being located between 50 and 65 °C, with a weight loss ranging between 2 and 11% and the overall E_a ranging between 10.5 and 65.5 kJ mol^{-1} (Table 2). Although the samples were sufficiently dried before measurements, the water molecules which are bound to polymer molecules through hydrogen bonds did not evaporate. The weight loss was smaller when the samples were previously treated at 150 °C, this could be an evidence of the water loss during the heat-induced reaction, which implies the amide bonds formation. A higher weight loss was observed when PVA was used as polycation, for the same polyelectrolyte concentration, probably due to its higher water-retention capacity. At higher polyions concentration, the higher amount of polymers adsorbed on silica particles was enough to reveal a second degradation step in the range 125–305 °C, assigned to the thermal degradation of polymer components.

In order to obtain information about the type of the degradation mechanism, the dependency of the activation energy versus conversion degree (α, where $\alpha = W_t/W_\infty$ with W_t—weight loss at the "t" moment of the process and W_∞—final weight loss of the decomposition step), by applying Reich–Levi method [38] on the entire variation

Table 2 TGA parameters of some multilayer/silica samples before and after the thermal treatment

Sample	Concentration (M)	Temperature range (°C)	T_m^a (°C)	w^b (%)	n^c	E_a^d (kJ mol^{-1})
$(PAEA/PAA)_2$	10^{-2}	20–160	50	3	1.5	26.6
$(PAEA/PAA)_2$, 150 °C	10^{-2}	20–270	53	2	1.2	10.5
$(PVA/PAA)_2$	10^{-2}	20–120	65	11	1.7	65.5
$(PVA/PAA)_2$, 150 °C	10^{-2}	20–120	48	3	1.2	28.6
$(PVA/PAA)_2$	5×10^{-2}	20–125	60	3	1.8	43.1
		125–305	220	3	1.2	67.4
$(PVA/PAA)_2$, 150 °C	5×10^{-2}	20–215	72	2	1.8	24.0

[a] Temperature corresponding to the maximum rate of decomposition

[b] The weight loss

[c] The reaction order

[d] The activation energy

field of the conversion degree has been determined. The Reich and Levi method is an integral method for the determination of the activation energy by the relation (3):

$$E_a = \frac{\ln \frac{A_{I+II}}{A_I}}{R\left(\frac{1}{T_I} - \frac{1}{T_{II}}\right)} \quad (3)$$

where A is the area comprised between the curve $\alpha = f(T)$, the temperature axis, and a line parallel with the coordinate axis corresponding to a constant temperature T_i, calculated with relations (4)

$$A_I = \int_0^{T_I} F(\alpha)\mathrm{d}T_i \text{ and } A_{I+II} = \int_0^{T_{I+II}} F(\alpha)\mathrm{d}T. \quad (4)$$

Figure 6 shows E_a versus α curves obtained for the first thermogravimetric step of the investigated samples.

In Fig. 6, the shape of the E_a–α plots is similar for the (polycation/PAA)$_2$/silica samples, irrespective of the polycation structure and concentration. At the same time, higher values of E_a were observed for PVA-based composites in this thermogravimetric stage, which shows that the amount of water adsorbed was higher than in the case of PAEA-based composites, supporting the differences between the weight losses values observed in the TG curves. Moreover, the continuous decrease of E_a values suggests that beside the loss of physical adsorbed water a chemical process takes place, which can be ascribed to elimination of water molecules from inter-layers ionic pairs and their transformation into covalent bonds. The shape of the E_a–α plots was completely different for the samples previously treated at 150 °C, almost unchanged E_a values being obtained when α ranged between 0.3 and 0.7%, for both polyelectrolyte concentrations. This suggested a continuous dehydration process, most probably due to the loss of the physically adsorbed water molecules, without any chemical reaction. Increasing the polyions concentration (Fig. 6b), a looser multilayer is probably formed, with a high capacity to eliminate the water molecules. Thus, smaller activation energies were necessary for this thermogravimetric process. The continuous decrease of E_a values with the increase of the conversion degree in the second thermal degradation step, observed for (PVA/PAA)$_2$/silica sample, with polyions adsorbed from 5×10^{-2} M solutions (the inset of 6b), suggests that the depolymerization is the main process in this stage.

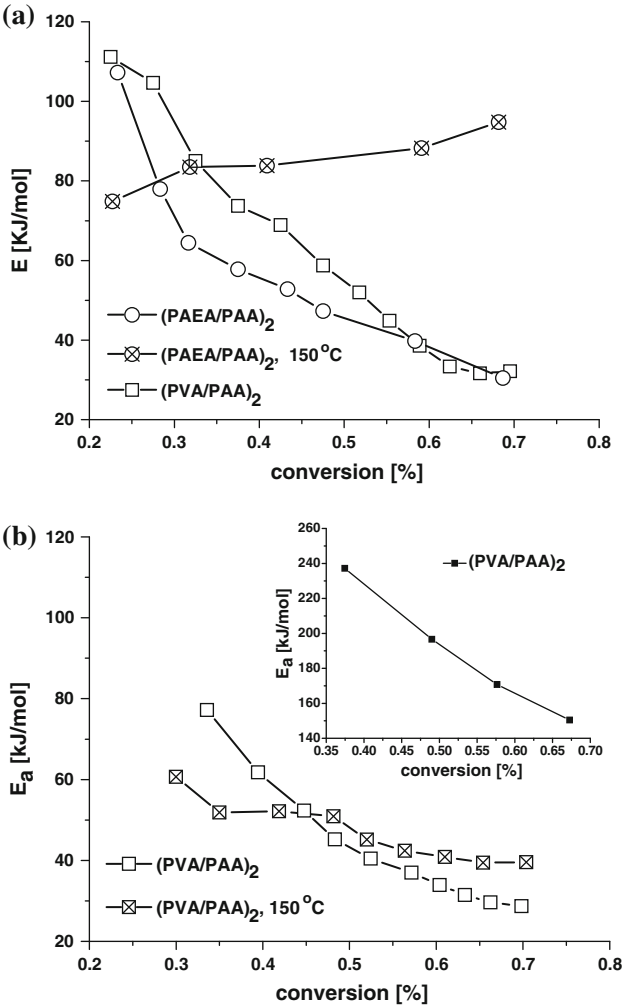

Fig. 6 The variation of activation energy (E_a) versus conversion degree (α), for the temperature range of 40–150 °C, for two concentrations of the adsorbed polymers: **a** 10^{-2} M and **b** 5×10^{-2} M. In *Inset* **b**, the temperature range is 125–300 °C

Dye adsorption on organic/inorganic composite materials

The multilayer/silica hybrids, having the polyanion or polycation as last adsorbed layer, were tested as sorbents for a cationic dye, MB, belonging to the phenothiazine family. The effects of the dye concentration and the structure of organic/silica materials on the CRE are shown in Table 3. The initial concentration of dye varied in the range 2×10^{-5} to 2×10^{-4} mol L^{-1}, and the contact time was fixed at 8 h.

In Table 3, the bare silica particles had weak adsorption capacity, the values of CRE being smaller than 30%, irrespective of MB initial concentration. As silica surface is negatively charged, the electrostatic adsorption of MB on the particles surface is the most probable process. The adsorption capacity increased significantly after the multilayer deposition and was strongly influenced by the nature of the last adsorbed layer. Thus, higher CRE values were obtained when PAA was the last adsorbed layer, suggesting that the adsorption of the cationic dye on the surface of the composite particles takes place by electrostatic interactions. When the polyelectrolytes were adsorbed from the concentrated solutions, the thicker adsorbed layers allowed

Table 3 Color removal efficiency, CRE, of some multilayer/silica samples before and after the thermal treatment

Sample	C^a (M)	T^b	C^c_{MB} (M)		
			2×10^{-4} CRE (%)	7×10^{-5}	2×10^{-5}
SiO_2		–	20.23	24.94	28.82
$+(PAEA/PAA)_2$	10^{-2}	–	42.69	65.15	85.90
$+(PAEA/PAA)_2$	5×10^{-2}	–	66.15	87.65	90.43
$+(PAEA/PAA)_2$	10^{-2}	150 °C	56.37	71.96	72.60
$+(PAEA/PAA)_{2.5}$	10^{-2}	–	21.28	36.07	59.65
$+(PAEA/PAA)_{2.5}$	5×10^{-2}	–	28.23	50.90	62.75
$+(PAEA/PAA)_{2.5}$	10^{-2}	150 °C	18.43	31.51	50.33

[a] Polyions adsorption concentration

[b] Thermal treatment

[c] Methylene blue concentration in the adsorption solution

a higher adsorption capacity of MB into the films. The thermal treatment of the composite materials increased the stability of the multilayer film, higher CRE values being obtained comparative with the non-thermal-treated composite materials. The smaller CRE values obtained at high MB concentration can be correlated with the aggregation of the dye molecules in concentrated aqueous solutions, which has as a consequence the limitation of dye adsorption into the organic films.

Conclusions

In this article, we report on the surface modification of silica particles by consecutive self-assembly of some weak polyelectrolytes, PVA, PAEA, and PAA, and the stabilization of the adsorbed films by annealing the multilayer/silica hybrids at 150 °C. The organic/silica composite properties were monitored by potentiometric titration, laser light scattering, infrared spectroscopy, and TGA. The thickness of the adsorbed layers depends on the polycation structure, thicker multilayer being adsorbed when the polycation with a higher spacer between the backbone and the ionic groups was used. The dye adsorption capacity of composite materials was strongly influenced by the nature of the last adsorbed layer. Higher CRE values were obtained when PAA was the last adsorbed layer, suggesting that the adsorption of cationic dye takes place on the composite particles mainly by electrostatic interactions.

The thermal treatment used to obtain composite materials with high stability, open large perspectives for the fabrication of complex three-dimensional hybrid nanostructures for various applications.

Acknowledgements The authors thank the group of Micro- and nano-structures characterization Laboratory ("Petru Poni" Institute of Macromolecular Chemistry, Iasi, Romania) for performing particle dimension measurements. The financial support of European Social Fund—"Cristofor I. Simionescu" Postdoctoral Fellowship Program (ID POSDRU/89/1.5/S/55216) and Grant No. 981 (Exploratory Research Project) is gratefully acknowledged.

References

1. Kelly A (2006) J Mater Sci 41:905. doi:10.1007/s10853-006-6569-9
2. Kuraoka K, Ueda T, Sato M, Okamoto T, Yazawa T (2005) J Mater Sci 40:3577. doi:10.1007/s10853-005-2880-0
3. Dorozhkin SV (2009) J Mater Sci 44:2343. doi:10.1007/s10853-008-3124-x
4. Loh KJ, Chang D (2011) J Mater Sci 46:228. doi:10.1007/s10853-010-4940-3
5. Decher G (1997) Science 27:1232
6. von Klitzing R, Tieke B (2004) Adv Polym Sci 165:177
7. Pallandre A, Moussa A, Nysten B, Jonas AM (2006) Adv Mater 18:481
8. Dragan ES, Mihai M, Schauer J, Ghimici L (2005) J Polym Sci A Polym Chem 43:4161
9. Kudaibergenov SE, Tatykhanova GS, Arinov BZh, Kozhakhmetov SK, Aseyev VO (2008) eXPRESS Polym Lett 2:101
10. Ai H, Gao J (2004) J Mater Sci 39:1429. doi:10.1023/B:JMSC.0000013910.63194.db
11. Fu H, Kobayashi T (2010) J Mater Sci 45:6694. doi:10.1007/s10853-010-4762-3
12. Dragan ES, Schwarz S, Eichhorn K-J (2010) Colloid Surf A 372:210
13. Fendler JH (1996) Chem Mater 8:1616
14. Mamedov A, Kotov NA, Prato M, Guldi DM, Wicksted JP, Hirsch A (2002) Nat Mater 1:190
15. Sukhishvili SA (2005) Curr Opin Coll Interface Sci 10:37
16. Serizawa T, Hamada K, Kitayama T, Fujimoto N, Hatada K, Akashi M (2000) J Am Chem Soc 122:1891
17. Caruso F, Furlong DN, Ariga K, Ichinose I, Kunitake T (1998) Langmuir 14:4559
18. Harris JJ, Bruening ML (2000) Langmuir 16:2006
19. Caruso F, Schüler C (2000) Langmuir 16:9595
20. Yang X, Johnson S, Shi J, Holesinger T, Swanson B (1997) Sens Actuator B Chem 45:87
21. Krasemann L, Tieke B (2000) Langmuir 16:287

22. DeLongchamp D, Hammond PT (2001) Adv Mater 13:1455
23. Sukhorukov GB, Antipov AA, Voigt A, Donath E, Mohwald H (2001) Macromol Rapid Commun 22:44
24. Shutava T, Prouty M, Kommireddy D, Lvov Y (2005) Macromolecules 38:2850
25. Tong W, Gao C, Mohwald H (2006) Macromolecules 39:335
26. Balachandra M, Dai J, Bruening ML (2002) Macromolecules 35:3171
27. Dragan ES, Mihai M, Airinei A (2006) J Polym Sci A Polym Chem 44:5898
28. Dragan S, Barboiu V, Petrariu I, Dima M (1981) J Polym Sci Polym Chem Ed 19:2869
29. Mastersizer 2000 brochure. http://www.malvern.com/common/downloads/MRK501.pdf
30. Bucatariu F, Dragan ES, Simon F (2007) Biomacromolecules 8:2954
31. Simon F, Dragan ES, Bucatariu F (2008) React Funct Polym 68:1178
32. Pretsch E, Bulmann P, Affolter C (eds) (2000) Structure determination of organic compounds. Tables of spectral data, 3rd edn. Springer-Verlag, Berlin, Heidelberg, New York, pp 245–312
33. Berwig E, Severgnini VLS, Soldi MS, Bianco G, Pinheiro EA, Pires ATN, Soldi V (2003) Polym Degrad Stab 79:93
34. Coats W, Redfern JP (1964) Nature 201:68
35. Hamciuc C, Vlad-Bubulac T, Petreus O, Lisa G (2007) Eur Polym J 43:980
36. Cai J, Bi L (2008) Integral Energy Fuels 22:2172
37. Stawski D, Jantas R (2009) Potato Res 52:355
38. Reich L, Levi DW (1963) Makromol Chem 66:102